

Negative oxygen vacancies in HfO_2 as charge traps in high-k stacks

J. L. Gavartin, D. Muñoz Ramo, A. L. Shluger

Department of Physics and Astronomy, University College London, Gower Street, London WC1E 6BT, UK

G. Bersuker and B. H. Lee

SEMATECH, 2706 Metropolis Dr., Austin, TX 78741, USA

(Dated: November 3, 2018)

We calculated the optical excitation and thermal ionization energies of oxygen vacancies in m- HfO_2 using atomic basis sets, a non-local density functional and periodic supercell. The thermal ionization energies of negatively charged V^- and V^{2-} centres are consistent with values obtained by the electrical measurements. The results suggest that negative oxygen vacancies are the likely candidates for intrinsic electron traps in the hafnium-based gate stack devices.

Hafnium based oxides are currently considered as a practical solution satisfying stringent criteria for integration of high-k materials in the devices in future technology nodes. However, high-k transistor performance is often affected by high and unstable threshold potential¹, V_t , and low carrier mobility². These effects are usually attributed to a high concentration of charge traps and scattering centers in the bulk of the dielectric and/or at its interface with the silicon channel. Although the reported trap densities vary greatly with fabrication techniques, the majority of data point to existence of a specific intrinsic shallow electron centre common to all HfO_2 based stacks while some extrinsic defects, such as Zr substitution in HfO_2 , have also been considered³.

Oxygen vacancies are dominating intrinsic defects in the *bulk* of many transition metal oxides including HfO_2 and ZrO_2 , and are thought to be also present in high concentrations in thin films. However, in spite of numerous experimental studies, evidence relating oxygen vacancies to measured characteristics of interface traps in high-k stacks is still mostly circumstantial. Therefore, accurate theoretical characterization of these defects is highly desirable.

Previous theoretical calculations of oxygen vacancy in HfO_2 and ZrO_2 reported the ground state properties obtained within local or semilocal approximations to density functional theory (DFT) methods (see^{4,5} for a review). This approach, however, significantly underestimates band gaps, which hampers determining energies of defect levels with respect to the band edges and precludes identifying shallow defect states^{5,6,7}. As a result, most of the early local DFT calculations (except, perhaps, ref.⁸) failed to predict unambiguously negative charge states of oxygen vacancy in HfO_2 . Significant improvement was achieved by Robertson *et al.*^{4,9,10} who used screened exchange approximation to predict vacancy energy levels including V^- charge state. However, these calculations were performed using a small periodic supercell and therefore corresponded to extremely high vacancy concentrations. The quality of the functional used is also largely unknown and needs independent verification.

In this work we used much bigger supercells and a non-local functional to calculate optical excitation and ther-

mal ionization energies of oxygen vacancies in five charge states. To relate these energies to experimental data we distinguish optical absorption/reflection type measurements involving Frank-Condon type (*vertical*) excitations, and electrical thermal de-trapping measurements, where phonon-assisted electron excitations are accompanied by strong *lattice relaxation*. We focus on the results of so called de-trapping electrical measurements^{11,12,13} which are interpreted in terms of thermal ionization of shallow electron traps and demonstrate that the interpretation is consistent with thermal ionization of negative V^- and V^{2-} vacancies.

Our periodic non-local density functional calculations were carried out using atomic basis set and a B3LYP hybrid density functional¹⁴ implemented in the CRYSTAL03 code¹⁵. This method reproduces band gaps of a range of transition metal oxides¹⁶ and allows us to carry out geometry optimization of defect structures, calculate defect electronic properties and excitation energies within the same method. We used all electron basis-set for oxygen atoms¹⁷, and an s,p,d valence basis set for Hf in conjunction with the relativistic small core effective potential due to Stevens *et al.*¹⁸. All calculations were carried out in the 96 atoms supercell of a monoclinic (m)- HfO_2 with a mesh of 36 k points in the irreducible Brillouin zone. The defect structures were optimized to the atomic forces below 0.03 eV \AA^{-1} . The compensating uniform background potential method was used for charged defects calculations^{6,19}. The positions of occupied and un-occupied single-electron defect levels in the gap of m- HfO_2 predicted by periodic B3LYP calculations are presented in Figure 1. The results of the calculations can be summarized as follows:

1. The calculated single-electron band gap in m- HfO_2 is 6.1 eV. We note, that single-electron estimate neglects excitonic effects, and effects of phonon broadening which reduce measured optical band gap of HfO_2 by 0.8 eV²⁰. Taking this into account, predicted E_g is in good agreement with the experimental optical gap of 5.6-5.9 eV²¹.
2. Oxygen vacancy in the monoclinic HfO_2 may exist in five charge states +2, +1, 0, -1, -2 corresponding to up to four extra electrons in the vicinity of the vacant O^{2-} site.

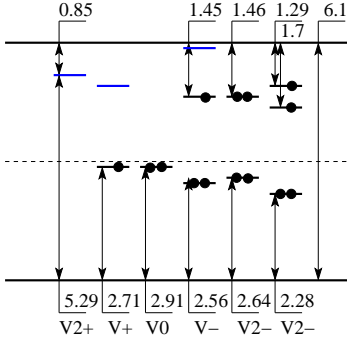


FIG. 1: Defect energy diagram for the 4-coordinated oxygen vacancy in the m-HfO₂.

3. The preferential site for the oxygen vacancy formation in m-HfO₂ depends on the charge state: V²⁺ and V⁺ are more stable in the 3-fold coordinated sites, whereas the V⁰, V⁻, and V²⁻ are energetically more favorable at the 4-fold coordinated sites (see also refs.^{5,22}). The difference in formation energies between 3- and 4-coordinated sites of negatively charged vacancies is about 0.2 eV.

4. The density of electrons in the +1 and zero charge vacancy is peaked at the vacant site with significant admixture of d-states of the nearest neighbor hafnium ions, similar to plane wave DFT calculations^{5,22}. The single-electron states of these electrons are located roughly in the middle of the gap (Fig. 1), significantly lower than those reported by Robertson^{4,9,10}

5. Both one and two extra electrons added to a neutral vacancy form more diffuse asymmetric states localized mainly on 3 (out of 4) Hf ions surrounding the vacancy. The ground state of the V²⁻ is spin singlet, which is 0.2 eV lower than the spin triplet configuration (cf. Fig. 1).

6. The change of the vacancy charge state is accompanied by significant displacements of the nearest neighbor (NN) Hf atoms and next shell of oxygen atoms (NNN) (see also ref.²²). The NN Hf ions displace from their perfect lattice position approximately symmetrically. This displacement is away from the V²⁺ and V⁺ by 11% and 5% of a typical Hf-O distance, but *towards* the V⁻ and V²⁻ by 4% and 8%, respectively. The displacements of the NNN oxygen ions are substantially smaller and directed away from the negative vacancies.

7. The character of electron density distribution, strong lattice relaxation and relatively shallow single-electron levels (Fig. 1) suggest that trapping of extra electrons in negative V⁻ and V²⁻ vacancies is essentially polaronic in nature. The third and fourth electrons induce strong lattice polarisation, which in turn, creates the potential well for these electrons. Now we discuss a relation between the single-electron spectrum of Fig. 1 and experimental trap ionization measurements. For optical type measurements, such as optical absorption, and reflection ellipsometry²³, using energy differences between single-electron levels can provide reasonable accuracy^{5,22}. The situation is different in electrical measurements, which

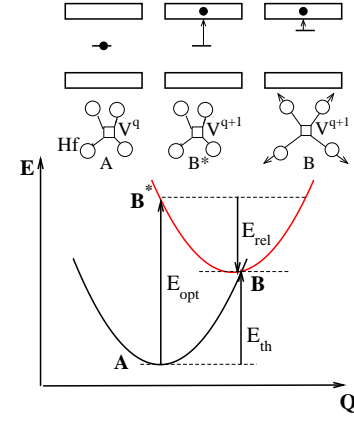


FIG. 2: Schematic potential energy surface (PES) for optical and thermal detrapping processes. Generalized displacement of the Hf atoms, Q, and energy scale is chosen to represent ionization of V²⁻ vacancy. The band diagram schematic illustrates optical and thermal ionization processes, respectively without (B*) and with (B) lattice relaxation.

include thermal excitation of trapped electrons into the conduction band of HfO₂¹¹ (see inset of Fig. 2).

The difference between the optical and thermal ionization can be qualitatively explained by the potential energy surface diagram depicted in Fig. 2 and earlier discussed for other systems (e.g. in ref.⁷). Fast optical ionization of a trap of charge q (state A) into the bottom of the conduction band (state B*) corresponds to a Frank-Condon type transition, E_{opt} , when no lattice relaxation associated with the removed charge occurs. In contrast, a much slower thermal ionization of a trap, E_{th} , is a phonon assisted process, during which the system transfers into a fully relaxed trap state $q+1$ and the electron delocalized at the bottom of the conduction band (state B). The ionized trap induces lattice polarization, which in case of the oxygen vacancy is mainly associated with strong displacements of the NN Hf ions. This generalized relaxation coordinate is denoted as Q in the diagram in Fig. 2. E_{th} is approximately given by:

$$E_{th} = E_{opt} - E_{rel}, \quad (1)$$

where E_{rel} is the lattice relaxation energy. Optical and thermal ionization energies can be calculated using the *total* energies of systems in different charge states as follows:

$$E_{opt}(V^q) = E_q(V^{q+1}) - E_q(V^q) + E^- - E^0; \quad (2)$$

$$E_{rel}(V^{q+1}) = E_{q+1}(V^{q+1}) - E_q(V^{q+1}). \quad (3)$$

The notations in Eqs. 2-3 have the following meaning: E^0 - the total energy of the perfect HfO₂ crystal; E^- - the total energy of the perfect HfO₂ crystal with an electron at the bottom of the conduction band; $E_q(V^q)$ - the total energy of HfO₂ with the vacancy in a charge state q ($q=+2,+1,0,-1,-2$) in the optimized geometry; $E_q(V^{q+1})$

TABLE I: Optical excitation energies, E_{opt} , relaxation energies, E_{rel} , and thermal activation Energies, E_{th} , for oxygen vacancies in m-HfO₂ calculated according to Eqs. 1-3.

q	E_{opt}	E_{rel}	E_{th}
V ⁺	3.33	1.01	2.32
V ⁰	3.13	0.80	2.33
V ⁻	1.24	0.48	0.76
V ²⁻	0.99	0.43	0.56

- the total energy of the vacancy in the charge state $q+1$ but at the equilibrium geometry corresponding to the vacancy in the charge state q . We assume that the vacancy is well separated from the interface, and the optical and relaxation energies discussed here, depend only on the bulk properties of HfO₂ and not on the Si or metal band alignment. The calculated values of E_{opt} , E_{rel} and E_{th} are summarized in Table I. We note that optical ionization energies, E_{opt} calculated as total energy differences in Eq. 2 are close to single-electron energy differences (Fig. 1). This is to be expected, since the total energy differences for the systems with N and N \pm 1 electrons in the DFT calculations are related to the single electron energies of the highest occupied and lowest unoccupied states²⁴.

The thermal ionization energies E_{th} are, however, 0.5

to 1.0 eV *smaller* than the optical energies due to the large lattice relaxation associated with the change of the charge state of the vacancy. Although the single particle energies of V⁻ and V²⁻ are very similar (Fig. 1), thermal ionization energies of these defects differ by 0.2 eV. These values are consistent with 0.35, 0.5 eV activation energies extracted from thermal de-trapping kinetics measurements^{11,12,13}. On the other hand, very large de-trapping energies for the V⁺ and V⁰ vacancies rule out these species as possible shallow electron traps. We should note that accounting for the thermal broadening of the defect levels and band tails, which will be discussed elsewhere, would improve the agreement between the calculated thermal ionization energies and the experimental energies even further.

To summarize, we have calculated the positions of single-electron levels for five charge states of oxygen vacancy in m-HfO₂ and related them to the existing experimental data. The results of trap discharging measurements^{11,12,13} are consistent with thermal ionization of negatively charged V⁻ and V²⁻ oxygen vacancies. These results further support the common assumption that oxygen vacancies are likely candidates for intrinsic electron traps in these devices and suggest that negative oxygen vacancies can be responsible for V_t instability.

-
- ¹ C. D. Young, G. Bersuker, G. A. Brown, P. Lysaght, P. Zeitzoff, R. W. Murto, and H. R. Huff, in *IEEE International Reliability Physics Symposium* (Phoenix, AZ, 2004), pp. 597–598.
 - ² R. J. Carter, E. Cartier, A. Kerber, L. Pantisano, T. Schram, S. De Gendt, and M. Heyns, *Appl. Phys. Lett.* **83**, 533 (2003).
 - ³ G. Bersuker, B. Lee, H. Huff, J. Gavartin, and A. Shluger, in *Defects in Advanced High-k Dielectric Nano-Electronic Semiconductor Devices*, edited by E. Gusev (Springer, 2006), pp. 227–236.
 - ⁴ J. Robertson, *Rep. Prog. Phys.* **69**, 327 (2006).
 - ⁵ A. L. Shluger, A. S. Foster, J. L. Gavartin, and P. V. Sushko, in *In Nano and Giga Challenges in Microelectronics*, edited by J. Greer, A. Korkin, and J. Labanowski (Elsevier, 2003), pp. 151–222.
 - ⁶ J. Gavartin, A. S. Foster, G. I. Bersuker, and A. L. Shluger, *J. Appl. Phys.* **97**, 053704 (2005).
 - ⁷ C. G. Van de Walle, *J. Appl. Phys.* **95**, 3851 (2004).
 - ⁸ C. Shen, M. F. Li, X. P. Wang, H. Y. Yu, Y. P. Feng, A. T. L. Lim, Y. C. Yeo, D. S. H. Chan, and D. L. Kwong, in *IEEE International Electron Devices Meeting* (2004), p. 733.
 - ⁹ K. Xiong and R. J., *Microelectronics Eng.* **80**, 408 (2005).
 - ¹⁰ K. Xiong, J. Robertson, M. C. Gibson, and S. G. Clark, *Appl. Phys. Lett.* **87**, 183505 (2005).
 - ¹¹ G. Bersuker, J. Sim, C. S. Park, C. Young, S. Nadkarni, R. Choi, and B. H. Lee, in *IEEE International Reliability Physics Symposium* (2006), pp. 179–183.
 - ¹² G. Ribes, J. Mitard, M. Denais, S. Bruyere, F. Monsieur, C. Parthasarathy, E. Vincent, and G. Ghibaudo, *IEEE Trans. Dev. Materials Reliability* **5**, 5 (2005).
 - ¹³ G. Bersuker, J. H. Sim, C. D. Young, C. S. Park, R. Choi, P. M. Zeitzoff, G. A. Brown, B. H. Lee, and R. Murto, *Microel. Reliability* **44**, 1509 (2004).
 - ¹⁴ A. D. Becke, *J. Chem. Phys.* **98**, 1372 (1993).
 - ¹⁵ V. Saunders, R. Dovesi, C. Roetti, R. Orlando, C. M. Zicovich-Wilson, N. M. Harrison, K. Doll, B. Civalieri, B. Bush, and P. L. M. D’Arco, *CRYSTAL 2003 User’s Manual* (University of Torino, 2003).
 - ¹⁶ F. Cora, M. Alfredsson, G. Mallia, D. S. Middlemiss, W. C. Mackrodt, R. Dovesi, and R. Orlando, *Structure and Bonding* **113**, 171 (2004).
 - ¹⁷ www.crystal.unito.it/Basis_Sets/ptable.html (????).
 - ¹⁸ W. J. Stevens, H. Basch, and P. Jasien, *Can. J. Chem.* **70**, 612 (1992).
 - ¹⁹ M. Leslie and M. J. Gillan, *J. Phys. C: Solid State Phys.* **18**, 973 (1985).
 - ²⁰ S. Sayan, T. Emge, E. Garfunkel, X. Zhao, L. Wielunski, D. Vanderbilt, J. S. Suehle, S. Suzer, and M. Banaszak-Holl, *J. Appl. Phys.* **96**, 7485 (2004).
 - ²¹ V. V. Afanas’ev and A. Stesmans, in *High-k Dielectrics*, edited by M. Houssa (IOP Publishing, Bristol and Philadelphia, 2004), pp. 217–250.
 - ²² A. S. Foster, F. Lopez Gejo, A. L. Shluger, and R. M. Nieminen, *Phys. Rev B* **65**, 174117 (2002).
 - ²³ H. Takeuchi, D. Ha, and T.-K. King, *J. Vac. Sci. Technol. A* **22**, 1337 (2004).
 - ²⁴ L. Kantorovich, *Quantum theory of solid state: An introduction* (Kluwer, 2004).